

# Three-dimensional Petersen-torus network: a fixed-degree network for massively parallel computers

Jung-hyun Seo

Published online: 3 November 2011  
© Springer Science+Business Media, LLC 2011

**Abstract** A two-dimensional (2D) Petersen-torus network is a mesh-class fixed-degree network designed using a Petersen graph, which has a maximum of 10 nodes when the degree is 3 and the diameter is 2 in a  $(d, k)$ -graph problem. Here, I propose a new three-dimensional (3D) Petersen-torus network that extends the 2D Petersen-torus network without increasing the degree. The 3D Petersen-torus has the same number of nodes ( $N$ ). The 3D Petersen-torus is better than the well-known 3D torus and 3D honeycomb mesh in terms of diameter and network cost. The 3D Petersen-torus network is better than the hypercube-like and star graph-like networks in terms of extendibility. Hence, the proposed network may serve as the foundation for realizing a high-performance multicomputer. In this paper, the optimal routing algorithm, Hamilton cycle, and several basic attributes are discussed. Furthermore, a comparison with a mesh-class fixed-degree 3D network is made for degree, diameter, and network cost.

**Keywords** Multicomputer · Interconnection network · 3D Petersen-torus · Petersen graph · Routing

## 1 Introduction

Over the past years, High Performance Computing (HPC) has been extensively studied by researchers and applied to a variety of fields ranging science, engineering, and business. With the development of HPC, there are many computing paradigms including multicomputer, multiprocessor, Grid computing, Cloud computing, Peer-to-Peer (P2P) computing, etc. [1]. The interconnection network (methods of interconnecting processors) plays a critical role in improving the system performance of

---

J.-h. Seo (✉)  
Department of Computer Engineering, National University of Suncheon, Suncheon, Jeonnam,  
Republic of Korea  
e-mail: [jhseo@scnu.ac.kr](mailto:jhseo@scnu.ac.kr)

a multicomputer. Hence, the interconnection network is a performance-determining factor. A great deal of research on multicomputer has dealt with interconnection networks to achieve goals such as low latency, high bandwidth, and low hardware cost. The performance of multicomputer can be improved with advancements in hardware implementation technology, routing schemes, data/task distribution, and many other application parameters. Nevertheless, their performance is most likely to be affected by interconnection network because technology, distribution, schema, and application parameters are all affected by the interconnection network. Researchers of multicomputer are thus motivated to propose new or improved interconnection networks [2].

An interconnection network defines the linking structure among processors, which is expressed in a graph with nodes corresponding to the processor and edges corresponding to the communication link. The number of edges combined with a node is called the degree. The minimum number of edges between two nodes is called the distance, and the maximum distance within a network is called the diameter. Network cost is a product of degree and diameter and is an important measure for the evaluation of interconnection networks. Degree and diameter trade off with each other. The diameter indicates the worst-case number of hops required for sending a message from one node to another. It is obvious that the worst-case latency for messages in a network with store-and-forward routing is highly dependent on the diameter. In wormhole routing [3] networks with large diameters, the worms tend to be longer and thus occupy a greater portion of the aggregate network bandwidth. This either increases the possibility of deadlock or else forces us to use less aggressive routing algorithms [4]. It can be said that when several interconnection networks have the same number of nodes, the network with the lowest cost is the most advantageous. The importance of diameter and network cost is described in [5].

Interconnection networks are classified into hypercube-like [6] and star graph-like [7] networks, where the degree increases in proportion to the number of nodes whenever the network is extended; on the other hand, in mesh-like [8] networks, the degree is constant even when the network is extended. Other such include Cayley graph networks [9, 10], Cartesian product networks [11] and Hierarchical networks [12]. The fixed-degree network is not necessary adding routing channel whenever the network is extended. But hypercube-like and star graph-like networks are necessary. For this reason, fixed-degree networks' extensibility is better than the others. In the case of hypercube-like and star graph-like networks, the diameter does not increase greatly with the degree, which increases whenever the network is extended. On the other hand, in the case of mesh-like networks, the degree is fixed, and therefore, the diameter increases whenever the network is extended.

In store-and-forward communication, where the latency time between two nodes is sensitive to the distance, a hypercube-like or star graph-like network with a short diameter is suitable. Store-and-forward routing was used in the first generation hypercubes. Hypercube-like networks include hypercube [6], folded hypercube [13], multiply twisted cube [14], and recursive circulant [15], and they are commercially available as iPSC/2, iPSC/860, n-CUBE/2, etc. [6]. Star graph-like networks include star graph [7], macro-star [16], transposition graph [17], and matrix-star graph [18]. Since the early 1990s, the two-dimensional (2D) mesh has become popular due to its simplicity and efficiency. Mesh-like networks include torus [8], honeycomb mesh

[19], diagonal mesh [8], and hexagonal mesh [20], and they are commercially available as MasPar Intel Paragon, XP/S, Touchstone DELTA System, and Mosaic C [21]. 2D mesh-like networks are designed by successively extending polygons along a plane, e.g., triangle, quadrangle, etc. In wormhole communication, where the latency time between two nodes is insensitive to the distance, mesh-like network with a large diameter is suitable. Recently, since it achieves a significant reduction in communication delay, the three-dimensional (3D) torus has emerged as a new candidate interconnection network for multicomputer. Wormhole routing technology has been widely used in new-generation multicomputer networks. 3D mesh-like networks are designed by laying these 2D networks above and under the space. 3D mesh-like networks include 3D mesh, 3D torus [22], 3D hexagonal mesh [21], 3D honeycomb mesh [23], and diamond networks [2]; several 3D mesh-like networks have been described in [24], and they are commercially available as Cray T3D, XT3 [25], XT4 [26], MIT's J-Machine, Tera Computer, etc. [27].

A 2D Petersen-torus (PT) [28] is a mesh-like network with a fixed degree and is designed using a Petersen graph with the optimal degree and diameter when the number of nodes is 10 in a  $(d, k)$ -problem. 2D PT is more advantageous in terms of network cost and bisection width than other mesh-like networks, and there have been studies on broadcasting and embedding with other networks [29–31]. In this study, the 3D PT is designed by laying a 2D PT above two or more spaces. The diameter edge of the 2D PT is removed and is linked to the nodes of a different 2D PT. In this manner, a 3D PT with degree 4 is designed using a 2D PT; thus, it is a cost-effective network. To illustrate the findings of this study, a comparison of the network cost and diameter is shown in Table 1 for a 3D honeycomb mesh having the same number of nodes as the 3D PT network and a 3D hexagonal mesh. In this paper, the Relevant Studies section describes the routing of the Petersen graph, the nature of the Hamiltonian path for the Petersen graph, and the 2D PT structure. The 3D PT( $l, m, n$ ) Network section suggests a 3D PT network and describes the optimal routing algorithm, Hamilton cycle, and several basic topological attributes. In addition, a comparison is made with a similar fixed-degree 3D network in terms of degree, diameter, and network cost. Finally, the conclusions are presented.

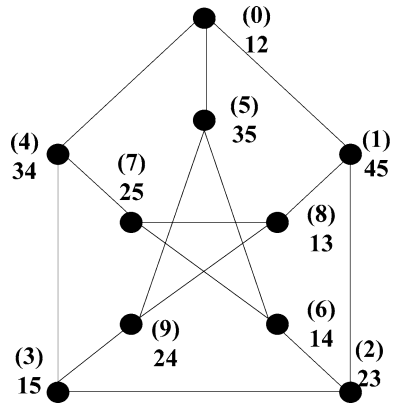
## 2 Relevant studies

### 2.1 Petersen graph

The Petersen graph incorporates a regular graph and a node(edge)-symmetric graph. It has a degree of 3, diameter 2, connectivity 3, and girth 5 [32]. There are several ways to assign node addresses. In the routing algorithm of the Petersen graph in the Relevant Studies section, an address consisting of permutations of double digits is used; in the PT network in the 3D PT( $l, m, n$ ) Network section, for convenience in indicating the node address, an address consisting of single digits in parentheses is used. The Petersen graph is shown in Fig. 1.

In the Petersen graph,  $P = (Vp, Ep)$ .  $x, y \in \{1, 2, 3, 4, 5\}$ ,  $x < y$ ,  $x', y' \in \{\{1, 2, 3, 4, 5\} - \{x, y\}\}$ ,  $x' < y'$ . The meaning of  $x, y \in \{1, 2, 3, 4, 5\}$  is “ $x$  and  $y$  is the

**Fig. 1** Petersen graph



elements of set  $\{1, 2, 3, 4, 5\}''$ . Node  $Vp = xy$ . Edge  $Ep = (xy, x'y')$ . It is assumed that in the Petersen graph, node  $U = u_1u_2$  (for example  $U = 12$ ) is a start node and node  $V = v_1v_2$  (for example  $V = 23$ ) is a destination node. The routing algorithm from  $U$  to  $V$  is as given below.

- Lemma 1** (Case 1) *If  $\{u_1, u_2\} \cap \{v_1, v_2\} = \emptyset$ ,  $U$  is adjacent to  $V$ .*
- (Case 2) *If  $\{u_1, u_2\} \cap \{v_1, v_2\} \neq \emptyset$ , it reaches  $V$  via the node composed of  $\{1, 2, 3, 4, 5\} - (\{u_1, u_2\} \cup \{v_1, v_2\})$  from  $U$ .*

**Lemma 2** *There is a Hamilton path starting from a node to reach the start node and all nodes except three nodes adjacent to the start node [32].*

2.2 2D PT( $m, n$ )

2D PT( $m, n$ ) is a regular graph with  $10mn$  as the number of nodes,  $20mn$  as the number of edges, 4 as the connectivity, and 4 as the degree. 2D PT is designed in such a way that it replaces the Petersen graph with the nodes of the torus, and this method is similar but not identical to that of making product networks. The degree of the product network is the sum of the degrees of the two networks, but the Petersen-torus is the Petersen graph + 1. The definition of 2D PT is as follows.  $PT(m, n) = (V_{pt}, E_{pt})$ .

$$V_{pt} = \{(x, y, p), 0 \leq x < m, 0 \leq y < n, 0 \leq p \leq 9\}$$

$E_{pt}$  is divided into internal edges and external edges. For internal edges, the edges of the Petersen graph are used as they are. Neighbor eight Petersen graphs are connected in a complete graph form by external edges. Two neighbor Petersen graphs that have the same  $y$ -axis value are connected by a horizontal edge. Two neighbor Petersen graphs that have the same  $x$ -axis value are connected by a vertical edge. Two neighbor Petersen graphs on a diagonal line are connected with a diagonal edge and a reverse diagonal edge. Two Petersen graphs, apart from each other by a distance of  $x + [m/2]$  and  $y + [n/2]$  diagonally, are connected by diameter edge.

The definition of a 2D PT network is omitted because it is nearly the same as that of 3D PT. Its detailed definition and characteristics are described in [28].

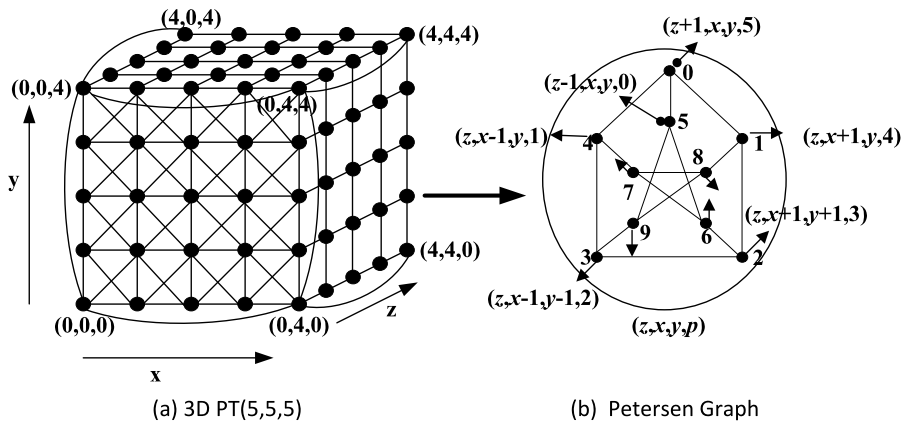


Fig. 2 3D Petersen-torus

### 3 3D PT(*l, m, n*) network

#### 3.1 Definition and attributes of the 3D PT(*l, m, n*) network

3D PT(*l, m, n*) (*l, m, n* ≥ 2) is formed by successively adding 2D PT toward the *z* axis. 3D PT(*l, m, n*) = (*Vpt, Ept*). The Petersen graph is set as a basic module, and the address of the basic module is indicated as (*z, x, y*), while the node address is indicated as (*z, x, y, p*). *z* is a coordinate of the *z* axis of the basic module, *x* is a coordinate of the *x* axis of the basic module, *y* is a coordinate of the *y* axis of the basic module, and *p* is the address of the node in the Petersen graph of the basic module. The node of 3D PT(*l, m, n*) is defined below.

$$Vpt = \{(z, x, y, p), \quad 0 \leq z < l, 0 \leq x < m, 0 \leq y < n, 0 \leq p \leq 9\}$$

The edge of 3D PT(*l, m, n*) is divided into an internal edge and an external edge, as mentioned below. Edges connecting the nodes belonging to the same basic module are called internal edges, and for internal edges, those of the Petersen graph are used as they are. Edges connecting nodes in different basic modules are called external edges, and are defined below. In the equations expressing the following edges, the symbol ‘/’ is a modulation operator.

- (1) The vertical edge is ((*z, x, y, 6*), (*z, x, (y + 1)/n, 9*))
- (2) The horizontal edge is ((*z, x, y, 1*), (*z, (x + 1)/m, y, 4*))
- (3) The diagonal edge is ((*z, x, y, 2*), (*z, (x + 1)/m, (y + 1)/n, 3*))
- (4) The reverse diagonal edge is ((*z, x, y, 7*), (*z, (x - 1 + m)/m, (y + 1)/n, 8*))
- (5) The dimensional edge is ((*z, x, y, 0*), ((*z + 1*)/*l, x, y, 5*))

Figure 2(a) is 3D PT(5, 5, 5), which indicates the basic module with points. A diameter edge in 2D PT is removed, and instead, a dimensional edge is added. The dimensional edge is ((*z, x, y, 0*), ((*z + 1*)/*l, x, y, 5*)). For neatness, in Fig. 2(a), wraparound edges are omitted at all basic modules. But wraparound edges are drawn at seven basic modules. In the basic module of 3D PT(*l, m, n*), nodes 1 and 4 are adjacent to horizontal edges, nodes 6 and 9 are adjacent to vertical edges, nodes 2 and 3

are adjacent to diagonal edges, nodes 7 and 8 are adjacent to reverse diagonal edges, and nodes 0 and 5 are adjacent to dimensional edges. The 3D PT( $l, m, n$ ) is a regular graph with  $10lmn$  as the number of nodes,  $20lmn$  as the number of edges, and 4 as the degree. Considering that the basic module is one node, it is node(edge)-symmetric and includes the 3D Torus. This characteristic simplifies the demonstration of the routing algorithm.

### 3.2 Simple routing algorithm

It is assumed that  $U(z, x, y, p)$  is the start node and  $V(z', x', y', p')$  is the destination node.  $dz = (z' - z + l)/l$ ,  $dx = (x' - x + m)/m$  and  $dy = (y' - y + n)/n$ .  $dm = \min(dx, dy)$  and  $dr = |dx - dy|$ .  $dz$  is the number of dimensional edges between the basic module to which the start node belongs and the basic module to which the destination node belongs.  $dx$  is the number of horizontal edges, and  $dy$  is the number of vertical edges.  $dm$  is the maximum available number of diagonal edges and  $dr$  is the number of extra horizontal or vertical edges. Given that a path from the start node to the destination node is  $P$ , a path at the start basic module of path  $P$  is  $SP$ , that at the destination basic module is  $DP$ , and another path other than  $SP$  or  $DP$  at path  $P$  is  $MP$ ; their lengths are  $lP, lSP, lDP$ , and  $lMP$ , in that order.  $lP = lSP + lDP + lMP$ . The aforementioned definition is used throughout this paper, including in the routing algorithm and [Appendix](#).

The routing algorithm matches the address of the start node  $U$  with that of the destination node  $V$ . The simple routing algorithm matches the addresses of the  $z, x$ , and  $y$  axes and  $p$ , in that order. This process is relatively simple, as shown below. In the following, only  $dz \leq l/2, dx \leq m/2$ , and  $dy \leq n/2$  are considered. If  $dz > l/2, dx > m/2$ , and  $dy > n/2$ , routing is performed in each opposite direction to the  $z, x$ , and  $y$  axes.

$$U(z, x, y, p) \rightarrow (z', x, y, 5) \rightarrow (z', x', y, 4) \rightarrow (z', x', y', 9) \rightarrow V(z', x', y', p')$$

Taking a closer look at it:

(1)  $U(z, x, y, p) \rightarrow (z', x, y, 5)$

$$U(z, x, y, p) \rightarrow (z, x, y, 0) \rightarrow (z + 1, x, y, 5) \rightarrow (z + 1, x, y, 0) \\ \rightarrow (z + 2, x, y, 5) \rightarrow \dots \rightarrow (z', x, y, 5)$$

(2)  $(z', x, y, 5) \rightarrow (z', x', y, 4)$

$$(z', x, y, 5) \rightarrow (z', x, y, 0) \rightarrow (z', x, y, 1) \rightarrow (z', x + 1, y, 4) \rightarrow (z', x + 1, y, 0) \\ \rightarrow (z', x + 1, y, 1) \rightarrow (z', x + 2, y, 4) \rightarrow \dots \rightarrow (z', x', y, 4)$$

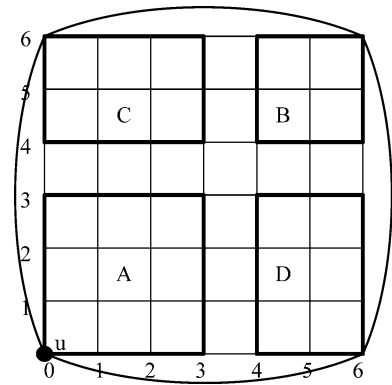
(3)  $(z', x', y, 4) \rightarrow (z', x', y', 9)$

$$(z', x', y, 4) \rightarrow (z', x', y, 7) \rightarrow (z', x', y, 6) \rightarrow (z', x', y + 1, 9) \\ \rightarrow (z', x', y + 1, 5) \rightarrow (z', x', y + 1, 6) \rightarrow (z', x', y + 2, 9) \\ \rightarrow \dots \rightarrow (z', x', y', 9)$$

(4)  $(z', x', y', 9) \rightarrow V(z', x', y', p')$

It is not necessary to explain this with the routing under Lemma 1.

**Fig. 3** Routing area in 2D  
PT(7, 7)



### 3.3 Optimal routing algorithm

The optimal routing algorithm minimizes the process of matching the addresses of the  $x$  and  $y$  axes in the simple routing algorithm. If  $dx = 4$  and  $dy = 5$ , in the simple routing algorithm, four horizontal edges and five vertical edges are used in the course of matching the addresses of the  $x$  and  $y$  axes. However, in the optimal routing algorithm, four diagonal edges and one vertical edge are used in the course of matching the addresses of the  $x$  and  $y$  axes. Additionally, the order of matching the  $x$ ,  $y$ , and  $z$  axes must be allowed for.

First of all, when two nodes are in the same two dimensions ( $x \neq x', y \neq y', z = z'$ ), the routing algorithm is examined and the time when they are in two different dimensions thereafter is examined. Lemmas 3, 4, and 5 used are as demonstrated in the Appendix.

#### 3.3.1 If $dz = 0$

In the routing algorithm, routing is done in four areas according to  $dx$  and  $dy$ , as shown in Fig. 3. In area A,  $dx \leq [m/2]$  and  $dy \leq [n/2]$ ; in area C,  $dx \leq [m/2]$  and  $dy > [n/2]$ ; in area D,  $dx > [m/2]$  and  $dy \leq [n/2]$ ; and in area B,  $dx > [m/2]$  and  $dy > [n/2]$ . If the destination node  $V$  is present in area B, move it symmetrically to the  $xy$  axis, if it is present in area C, move it symmetrically to the  $x$  axis, and if it is present in area D, move it symmetrically to the  $y$  axis; then it becomes the same as area A. That is, with regard to the routing algorithm of area A, routing shall be done just symmetrically to the  $x$  axis for area C, to the  $y$  axis for area D, and to the  $xy$  axis for area B. The optimal routing algorithm is dealt with only for area A.

The routing algorithm is divided into cases when the routing path is composed of one straight line and when it is composed of two straight lines. An exceptional case, in which the start node and the destination node are close to each other ( $dx, dy \leq 3$ ), shall be separately arranged. However, if the start basic module and the destination basic module are the same ( $dx = dy = 0$ ), routing is done under Lemma 1 and is omitted. The following is the optimal routing algorithm.

(Case 1)  $dx = dy$  or  $dx = 0$  or  $dy = 0$

#### 1.1 $dx = dy$

As in path A shown in Fig. 4, routing is done with a diagonal edge.

1.2  $dx = 0, dy \geq 4$

Between path A and path A' in Fig. 5, the shorter one is determined by Lemma 4.

1.3  $dx \geq 4, dy = 0$

This case represents when Case 1.2 is rotated by  $90^\circ$  in Fig. 5, and the figure is omitted; between path A and path A' using a diagonal edge, the shorter one is determined by Lemma 5.

(Case 2)  $dx, dy \geq 1, dr \geq 2$

2.1  $dx < dy$

Between path A and path B in Fig. 6, the shorter one is determined by Lemma 4.

2.2  $dx > dy$

This case represents when Case 2.1 is rotated by  $90^\circ$  in Fig. 6, and the figure is omitted; between path A and path B in Fig. 6, the shorter one is determined by Lemma 5.

(Case 3)  $dx, dy \leq 3$  (if the start node and the destination node are very close to each other)

3.1  $dx = 0, 1 \leq dy \leq 3$

The routing path is as shown in Figs. 7 and 8.

3.2  $dy = 0, 1 \leq dx \leq 3$

Change  $x$  and  $y$  in Case 3.1.

3.3  $dr = 1, dx > dy$

Between path A' and path B' in Fig. 6, the shorter one is determined by Lemma 4.

3.4  $dr = 1, dx < dy$

Change  $x$  and  $y$  in Case 3.3.

### 3.3.2 Demonstration

(Case 1)  $dx = dy$  or  $dx = 0$  or  $dy = 0$

1.1  $dx = dy$

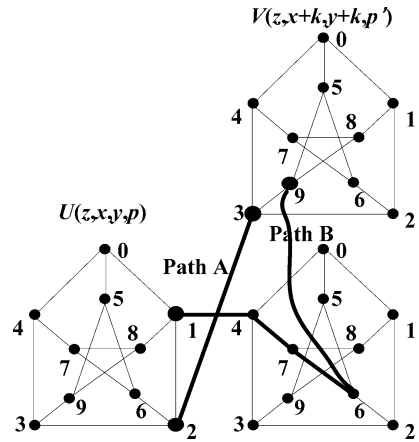
As in path A shown in Fig. 4, routing is done with a diagonal edge.

In Fig. 4,  $lMA = dm + dm - 1 = 2dm - 1$  and  $lMB = 2(dm + 2(dm - 1)) + 2 = 6dm - 2$ . If  $dm \geq 1$ , then  $lMA < lMB + 3$ . Since nodes 1 and 2 are adjacent to each other,  $lSA \leq lSB + 1$ , and since nodes 3 and 9 are adjacent to each other,  $lDA \leq lDB + 1$ . Thus,  $lA < lB$ .

For example, when  $dm = dx = dy = 1$ ,  $lMA = 1$  and  $lMB = 4$ . When  $q = 0$  and  $q' = 9$ ,  $lSA = 2$ ,  $lSB = 1$ ,  $lDA = 2$ , and  $lDB = 1$ .  $lA = 5$  and  $lB = 6$ . In this case,  $lA$  is less than  $lB$ , even when  $lA$  is the largest and  $lB$  is the smallest.



**Fig. 4** Routing path for  $dx = dy$



1.2  $dx = 0, dy \geq 4$

Between path A and path A' in Fig. 5, the shorter one is determined by Lemma 4.

Part (a) in Fig. 5 includes the condition that  $dy$  is an even number; for part (b),  $dy$  is an odd number. First, in Case (a), when  $dy$  is an even number,  $IMA = dy + (dy - 1) + 2 = 2dy + 1$  and  $IMB = dy + (dy - 1 - 3) + (2 \times 3) = 2dy + 2$ .  $ISA = ISB$  and  $IDA = IDB$ , so if  $dy \geq 4$ , then  $IMA < IMB$ .  $IMC = dy + 2(dy - 1) = 3dy - 1$ . If  $dy \geq 4$ , then  $IMA \leq IMC + 2$ . Nodes 2 and 6 are adjacent to each other, so  $ISA \leq ISC + 1$ , and nodes 8 and 9 are also adjacent to each other, so  $IDA \leq IDC + 1$ . Therefore,  $IA \leq IC$ . Likewise,  $IA' < IB'$  and  $IA' \leq IC$ . As mentioned in Lemma 3,  $IMA = IMA'$ . The lengths of path A and path A' are as mentioned in Lemma 4. In Case (b), when  $dy$  is an odd number,  $IMA = dy + (dy - 3) + (2 \times 2) = 2dy + 1$  and  $IMB = dy + (dy - 1 - 4) + (2 \times 4) = 2dy + 3$ .  $ISA = ISB$  and  $IDA = IDB$ , so if  $dy \geq 5$ , then  $IMA \leq IMB + 2$ .  $IMC = dy + 2(dy - 1) = 3dy - 1$ . If  $dy \geq 5$ , then  $IMA \leq IMC + 3$ . Nodes 2 and 6 are adjacent to each other, so  $ISA \leq ISC + 1$ , and nodes 8 and 9 are adjacent to each other, so  $IDA \leq IDC + 1$ . Therefore,  $IA \leq IC$ . Likewise,  $IA' < IB'$  and  $IA' \leq IC$ .  $IMA = IMA'$ . The lengths of path A and path A' are as mentioned in Lemma 4.

1.3  $dx \geq 4, dy = 0$

This case represents when Case 1.2 is rotated by  $90^\circ$  in Fig. 5, and the figure is omitted; between path A and path A' using a diagonal edge, the shorter one is determined by Lemma 5.

The result of Case 1.3 is the same as that of Case 1.2, with the exception that Case 1.2 is rotated by  $90^\circ$  toward the right. Only for the start basic module, the node adjacent to path A is 8 and that adjacent to path A' is 2; in the destination basic module, the node adjacent to path A is 3 and that adjacent to path A' is 7. As mentioned in Lemma 3,  $IA(= IA') < IB(= IB')$  and  $IA(= IA') \leq IC$ .  $IMA = IMA'$ . The lengths of path A and path A' are as mentioned in Lemma 5.

(Case 2)  $dx, dy \geq 1, dr \geq 2$

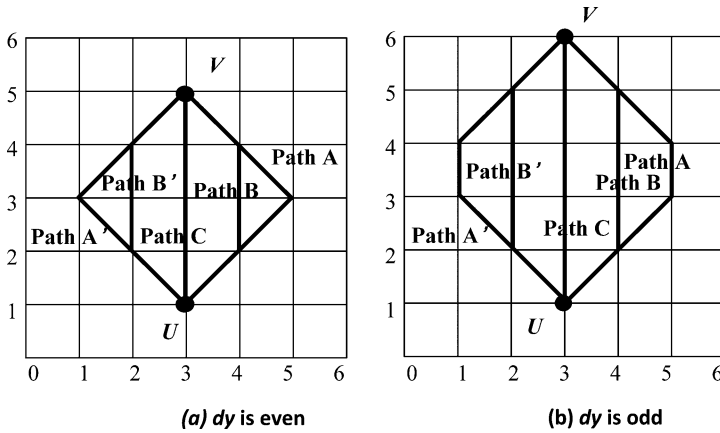
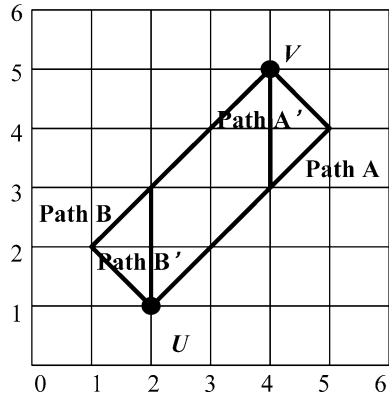


Fig. 5 Routing path for  $dy \geq 4, dx = 0$

Fig. 6 Routing path for  $dr \geq 2, dy \neq 0$



2.1  $dx < dy$

Between path A and path B in Fig. 6, the shorter one is determined by Lemma 4.

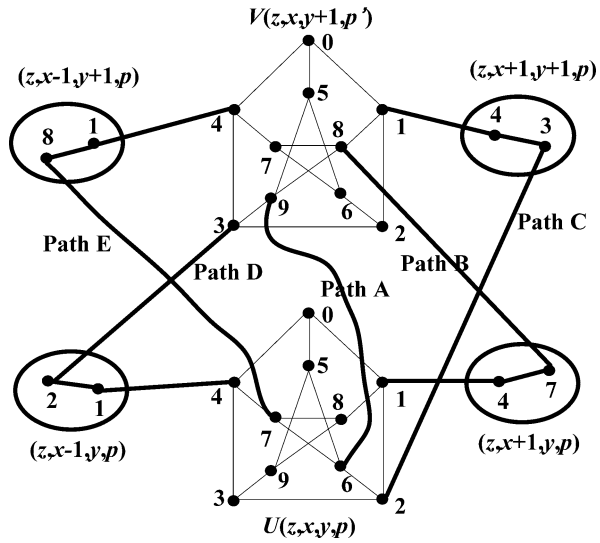
In Fig. 6,  $IMA = dy + dy - 2 + 2 = 2dy$  and  $IMA' = dy + dy - 3 + 2dr = 2(dy + dr) - 3$ . If  $dr \geq 2$ , then  $IMA \leq IMA' - 1$ .  $ISA = ISA'$  and nodes 2 and 6 are adjacent to each other, so  $IDA \leq IDA' + 1$ . Therefore,  $IA \leq IA'$ . The same applies to path B and path B'. The lengths of paths A, A', B and path B' are as mentioned in Lemma 4.

2.2  $dx > dy$

This case represents when Case 2.1 is rotated by  $90^\circ$  in Fig. 6, and the figure is omitted; between path A and path B in Fig. 6, the shorter one is determined by Lemma 5.

The result of Case 2.2 is the same as that of Case 2.1, with the exception as shown in Fig. 7, Case 2.2 is symmetrical to it from  $45^\circ$ . For the start basic module, the node adjacent to path A is 2 and that adjacent to path B is 8, and for the destination basic module, the node adjacent to path A is 7 and that adjacent to path B is 8. As mentioned in Lemma 3,  $IA(= IA') < IB(= IB')$  and  $IA(= IA') \leq IC$ .  $IMA = IMA'$ . The lengths of path A and path B are as mentioned in Lemma 5.

**Fig. 7** Routing path for  $dx = 0$ ,  $dy = 1$



(Case 3)  $dx, dy \leq 3$  (if the start node and the destination node are very close to each other)

3.1  $dx = 0, 1 \leq dy \leq 3$

The routing path is as shown in Figs. 7 and 8.

This case is divided into  $dy = 1$  and  $dy = \{2, 3\}$  according to the value of  $dy$ .

$$dy = 1$$

In Fig. 7,  $l_{MA} = 1$  and  $l_{MB} = l_{MC} = l_{MD} = l_{ME} = 3$ . In path B,  $l_{SA} \geq l_{SB} + 2$  and  $l_{DA} \geq l_{DB} + 1$ . To meet  $l_B < l_A$ ,  $l_{SB}$  shall be 2 less than  $l_{SA}$  and  $l_{DB}$  shall not be larger than  $l_{DA}$ . Therefore, if  $q = 1$  and  $q' = \{1, 7, 8, \}$ , then  $l_B < l_A$ . Otherwise,  $l_B \geq l_A$ . In path C,  $l_{SA} \geq l_{SC} + 1$  and  $l_{DA} \geq l_{DC} + 2$ . To meet  $l_C < l_A$ ,  $l_{DC}$  shall be 2 less than  $l_{DA}$  and  $l_{SC}$  shall not be larger than  $l_{SA}$ . Therefore, if  $q = \{1, 2, 3\}$  and  $q' = 1$ , then  $l_C < l_A$ . Otherwise,  $l_C \geq l_A$ . As in path B, in path D, if  $q = 4$  and  $q' = \{2, 3, 4\}$ , then  $l_D < l_A$ . Otherwise,  $l_D \geq l_A$ . As in path C, in path E, if  $q = \{4, 7, 8\}$  and  $q' = 4$ , then  $l_E < l_A$ . Otherwise,  $l_E \geq l_A$ .

$$dy = \{2, 3\}$$

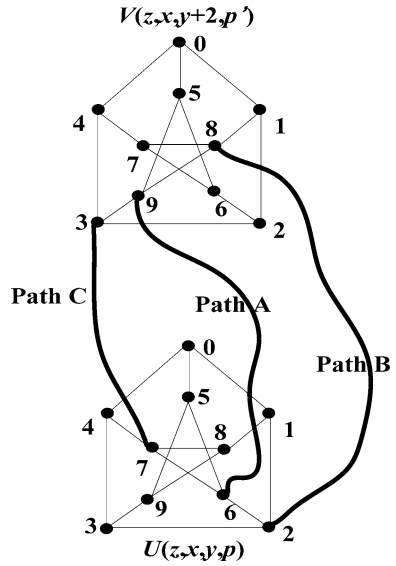
In Fig. 8,  $l_{MA} = l_{MB} = l_{MC}$ . The lengths of paths B and C, except path A, are as mentioned in Lemma 4, and the values of  $q$  are 5 and 6 so that  $l_{SA}$  can be 1 less than  $l_{SB}$  or  $l_{SC}$ ; the values of  $q'$  are 5 and 9 so that  $l_{DA}$  can be 1 less than  $l_{DB}$  or  $l_{DC}$ . Thus, if  $q = \{5, 6\}$  or  $q' = \{5, 9\}$ , then  $l_A \leq l_B$  and  $l_A \leq l_C$ . The remaining nodes are as mentioned in Lemma 4.

3.2  $dy = 0, 1 \leq dx \leq 3$

Change  $x$  and  $y$  in Case 3.1.

This case is obtained by rotating Case 3.1 by  $90^\circ$  to the right; it is divided into  $dx = 1$  and  $dx = \{2, 3\}$ , and the demonstration is omitted because it is the same as for Case 3.1.

**Fig. 8** Routing path for  $dx = 0$ ,  $dy = \{2, 3\}$



3.3  $dr = 1, dx > dy$

Between path A' and path B' in Fig. 6, the shorter one is determined by Lemma 4.

In this case,  $dr = 1$  in Case 2.1. In Fig. 7, of path A and path A', path A is negligible. Likewise, of path B and path B', path B is negligible.  $IMA' = IMB'$ . The lengths of path A' and path B' are as mentioned in Lemma 4.

3.4  $dr = 1, dx < dy$

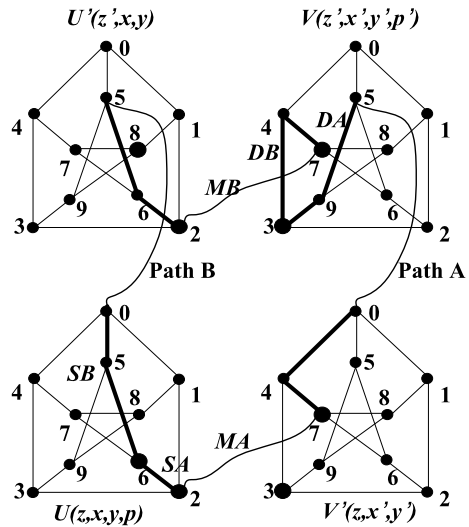
Change  $x$  and  $y$  in Case 3.3.

In this case, as in Case 3.3,  $dr = 1$  in Case 2.2. Of path A and path A', path A is negligible. Likewise, of path B and path B', path B is negligible.  $IMA' = IMB'$ . The lengths of path A' and path B' are as shown in Lemma 5.

3.3.3 If  $dz \neq 0$

In Fig. 9, it is assumed that the basic module having the same  $x$  and  $y$  values as the start basic module, as well as the same  $z$  value as the destination basic module, is  $U'$ , and the basic module having the same  $x$  and  $y$  values as the destination basic module, as well as the same  $z$  value as the start basic module, is  $V$ . In addition, it is assumed that length of the path from node  $U$  to node  $V'$  is  $IMA$  and that from node  $U'$  to node  $V$  is  $IMB$ . If  $dz = 0$ , then  $IMA = IMB$  according to the routing algorithm. Given that the length of the path from node  $U$  to node  $U'$  is  $IMDB$  and that from node  $V'$  to node  $V$  is  $IMDA$ ,  $IMDA = IMDB = dz + dz - 1$ . Therefore, assuming that the lengths of the internal path are  $IU'$  and  $IV'$  in  $U'$  and  $V$ , if  $ISA + IDA + IV' < ISB + IDB + IU'$ , then  $IA < IB$ . On the other hand, if  $ISA + IDA + IV' > ISB + IDB + IU'$ , then  $IA > IB$ . Therefore, if  $ISA + IDA + IV' < ISB + IDB + IU$ , routing shall be done with path A; otherwise, it shall be done with path B.

**Fig. 9** Routing path for  $dz \neq 0$



### 3.4 Diameter and bisection width

In Fig. 9,  $lMA = lMB$  and  $lMDA = lMDB = dz + dz - 1$ . Diameter in the Petersen graph is 2, so the maximum value of  $lSA + lDA + lV$  is 6. Diameter is  $\text{MAX}\{\text{MAX}(lA), \text{MAX}(lB)\}$ .  $\text{MAX}(lA) = lMA + lMDA + 6 = \text{MAX}(lB) = lMB + lMDB + 6$ . The maximum value of  $lMDA$  is obtained when  $dz = [l/2]$  and  $[l/2] + [l/2] - 1$ . The maximum value of  $lMA$  is obtained when  $dx = [m/2]$  and  $dy = 0$  or  $dx = 0$  and  $dy = [n/2]$ . The  $lMA$  values of the two cases are  $[m/2] + [m/2] - 1$  and  $[n/2] + [n/2] - 1$ . The maximum value of  $lMA$  is  $\text{MAX}([m/2] + [m/2] - 1, [n/2] + [n/2] - 1)$ . Therefore, the result shown in Theorem 1 is obtained.

**Theorem 1** *The diameter of 3D PT( $l, m, n$ ) is  $[l/2] + [l/2] - 1 + \text{MAX}([m/2] + [m/2] - 1, [n/2] + [n/2] - 1) + 6$ .*

When  $l = n = m$ , diameter  $k = [l/2] + [l/2] - 1 + \text{MAX}([m/2] + [m/2] - 1, [n/2] + [n/2] - 1) + 6 = 4[n/2] + 4$ . The diameter has different values according to whether  $n$  is an even number or an odd number; therefore, when it is arranged with a larger even number, the diameter is obtained as below.

**Corollary 1** *The diameter of 3D PT( $n, n, n$ ) is  $2n + 4$ .*

The bisection width is the least number of edges that need to be removed in order to separate network into two having the same number of nodes. The difference in the number of nodes of the two separated networks shall be 1 or less. If the bisection width is less, the network is only separated with fewer edge failures, so that it will fail to function well. A better effect can be generated with a larger bisection width. In brief, separating the 2D basic modules having a  $z, y$  value from those having a  $z - 1$  value is more effective than separating all layers consisting of two dimensions into

**Table 1** Diameter and network cost for 3d networks

Networks	Degree	Diameter	Network cost
3D Mesh	6	$3\sqrt[3]{N}$	$18\sqrt[3]{N}$
3D Torus	6	$1.5\sqrt[3]{N}$	$9\sqrt[3]{N}$
3D Prismatic Twisted Torus	6	$1.5\sqrt[3]{N/2}$	$9\sqrt[3]{N/2}$
3D Prismatic Doubly Twisted Torus	6	$1.5\sqrt[3]{N/2}$	$9\sqrt[3]{N/2}$
3D Hexagonal Mesh	8	$\approx 1.34\sqrt[3]{N} - 2$	$\approx 10.72\sqrt[3]{N} - 16$
3D Honeycomb Mesh	4	$\approx 3.63\sqrt[3]{N}$	$\approx 14.52\sqrt[3]{N}$
3D Petersen-torus	4	$0.92\sqrt[3]{N} + 4$	$3.68\sqrt[3]{N} + 16$

two. Additionally, the basic modules having a value of  $z + \lceil l/2 \rceil$  and those having a value of  $z - 1 + \lceil l/2 \rceil$  shall be separated. In order to separate the two-dimensional basic modules having a  $z$  value from those having a  $z - 1$  value,  $m \times n$  dimensional edges shall be removed. Therefore, the result shown in Theorem 5 is obtained.

**Theorem 2** *The bisection width of 3D PT( $l, m, n$ ) is  $2mn$ .*

When  $n = m$ ,

**Corollary 2** *The bisection width of 3D PT( $l, n, n$ ) is  $2n^2$ .*

In the following, a comparison is made between degree, diameter, and network cost when 3D networks with degree as a constant have the same number of nodes. The 3D PT has a shorter diameter and lower network cost than the other networks. In Table 1,  $N$  is the number of nodes.

The number of nodes for 3D mesh( $n, n, n$ ) is  $n^3$ , and the diameter is  $3n$ . The number of nodes for 3D torus( $n, n, n$ ) is  $n^3$ , and the diameter is  $1.5n$ . The number of nodes for a  $t$ -sized 3D honeycomb mesh is  $(32t^3 - 2t)/3$ , and the diameter is  $8t - 4$  [23]. The number of nodes for 3D Prismatic Twisted Torus( $2a, a, a$ ) is  $2a^3$ , and the diameter is  $3a/2$  [33]. The number of nodes for 3D Prismatic Doubly Twisted Torus( $2a, a, a$ ) is  $2a^3$ , and the diameter is  $3a/2$  [33]. The number of nodes for a  $t$ -sized 3D hexagonal mesh is  $10t^3/3 + 5t^2 + 11t/3 - 1$ , and the diameter is  $2(t - 1)$  [21]. The number of nodes for 3D PT( $n, n, n$ ) is  $10n^3$ , and the diameter is  $2n + 4$ .

### 3.5 Hamilton cycle

If a network has a Hamilton path or Hamilton cycle, it can readily implement a ring or linear arrangement; this is used as a pipeline and is very useful in parallel processing. If a Hamilton cycle exists on a node in a graph, the graph has a Hamilton cycle on all nodes, because a Hamilton cycle is a ring structure. In this paper, as shown in part (a) in Fig. 11, a Hamilton cycle starts from  $(0, 0, 0, 5)$  to reach  $(0, 0, 0, 5)$  via all nodes. Next is the Hamilton algorithm, as shown in Fig. 10 by steps. In the following, the paths among all nodes in the basic module, which are passed through in accordance with Lemma 2, are omitted.

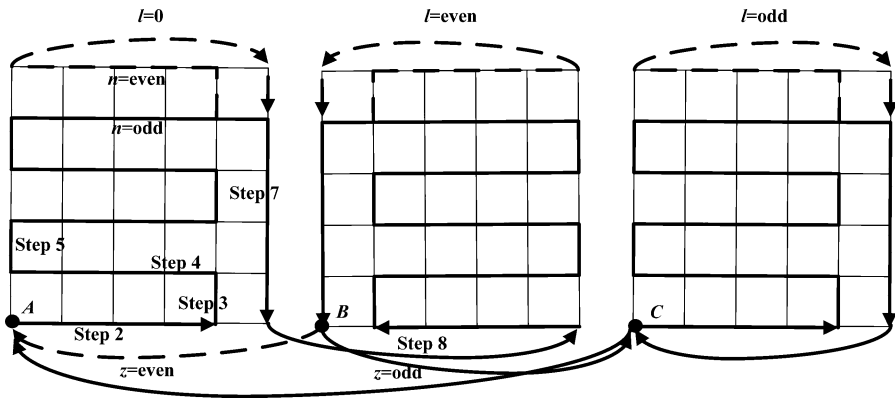


**Fig. 10** Hamilton cycle for 3D PT

- [Step 1] Start from node  $(0, 0, 0, 5)$ , move along nodes 9, 8, 7, 6, 2, 3, 4, 0, and 1 of the basic module  $(0, 0, 0)$  to reach node  $(0, 0, 0, 1)$ .
- [Step 2] If the  $y$  address value of the current node is  $n - 1$ , move to the  $(m - 1)$ th right basic module; otherwise, move to the  $(m - 2)$ th right basic module.
- [Step 3] If the  $y$  address value of the current node is  $n - 1$ , move to [Step 7]; otherwise, move to the upper basic module.
- [Step 4] If the  $y$  address value of the current node is  $n - 1$ , move to the  $(m - 1)$ th left basic module; otherwise, move to the  $(m - 2)$ th left basic module.
- [Step 5] If the  $y$  address value of the current node is  $n - 1$ , move to [Step 7]; otherwise, move to the upper basic module.
- [Step 6] Repeat [Step 2]–[Step 5].
- [Step 7] Move to the lower  $(n - 1)$ th basic module to reach node  $(0, m, 0, 6)$ .
- [Step 8] Start from node  $(0, m, 0, 6)$  to reach node  $(0, m, 0, 0)$  via nodes 5, 9, 8, 7, 4, 3, 2, and 1 of the same basic module.
- [Step 9] Start from node  $(0, m, 0, 0)$  to reach node  $(1, m, 0, 5)$ .
- [Step 10] Make [Step 8] symmetrical to the  $x$  axis at [Step 1] and repeat this process until it reaches node  $(1, 0, 0, 0)$ .
- [Step 11] If the  $z$  address value of the path is  $l - 1$ , it reaches the start node  $(0, 0, 0, 5)$  to complete the Hamilton cycle; otherwise, it reaches node  $(2, 0, 0, 5)$ .
- [Step 12] Reach node  $(2, 0, 0, 1)$  via nodes 6, 7, 8, 9, 3, and 2 of the same basic module in node  $(2, 0, 0, 5)$ .
- [Step 13] Repeat [Step 7] at [Step 1], and reach node  $(2, m, 0, 6)$ .
- [Step 14] Start from node  $(2, m, 0, 6)$  to reach node  $(2, m, 0, 1)$  via nodes 2, 3, 4, 7, 8, 9, 5, and 0 of the same basic module.
- [Step 15] Start from node  $(2, m, 0, 1)$  to reach the start node  $(0, 0, 0, 5)$  via node  $(2, 0, 0, 4)$  and node  $(2, 0, 0, 0)$ .

Figure 11 shows the Hamilton path in the basic modules A, B, and C in Fig. 10. In the basic module A, the initial start node is 5 and it moves from node 1 to node  $(0, 1, 0, 4)$ . It makes its rounds of all nodes and reaches node 5 from node  $(l, 0, 0, 0)$ . In the basic module B, it returns to node  $(z, 0, 1, 6)$  from node  $(z, 0, 1, 9)$ . If it makes its rounds of the last two dimensions at present, it returns to the start node  $(0, 0, 0, 5)$ ;

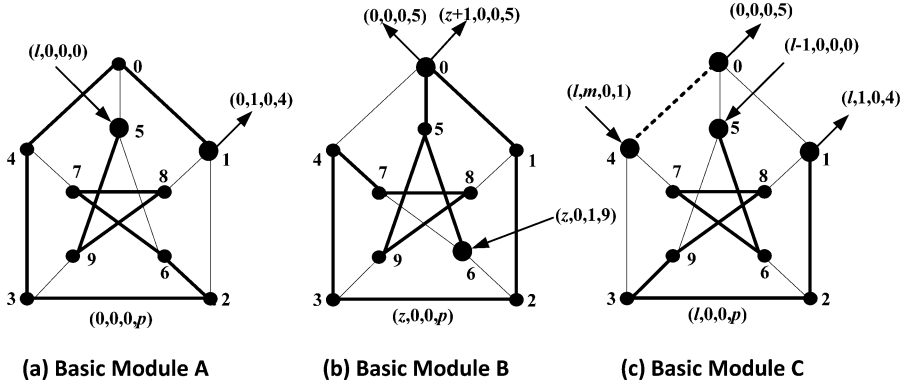


Fig. 11 Hamilton path for basic modules A, B, and C

otherwise, it returns to the  $(z + 1)$ -dimensional node  $(z + 1, 0, 0, 5)$ . If the last two dimensions'  $z$  value is an even number, it returns to the start node in the basic module B, and if it is an odd number, it passes through the basic module C. The basic module C is more complex. The path coming into node 5 from node  $(l - 1, 0, 0, 0)$  does not make its rounds of all nodes but, as shown in part (c) of the figure, goes out to node  $(l, 1, 0, 4)$  via nodes 5, 6, 7, 8, 9, 3, 2, and 1. The last path making its all rounds of all nodes on the condition of  $z = l$  returns to node 4 and enters the start node of the Hamilton path via node 5.

### 4 Conclusion

An effective interconnection network is a critical factor in the performance of large-scale parallel processing systems. Mesh-like, hypercube-like, and star graph-like interconnection networks that have typically been designed 3D interconnection networks, which extend mesh-like 2D interconnection networks to 3D, have also been developed. In this paper, a 3D PT was designed, an extension of a 2D PT. A 3D PT is effective in terms of network cost, because it is designed by replacing a diameter edge with a dimensional one without adding an edge when the 2D PT is extended, rather than by increasing the degree. In particular, in terms of network cost, for the same number of nodes ( $N$ ), the 3D PT has a value that is improved by four times in relation to the 3D mesh; two times, 3D torus; two times, 3D hexagonal mesh; and three times, 3D honeycomb mesh. The 3D PT is more advantageous than the 3D mesh or the torus networks in terms of the network cost. In relation to the limitation on the number of nodes when extending the network, it is better than both the 3D hexagonal mesh and the 3D honeycomb mesh. The Hamilton cycle algorithm developed in the designed network is available as a broadcasting and pipeline algorithm. However, using a Hamilton cycle to broadcast is inefficient. Therefore, a study on a new efficient broadcasting algorithm is required.



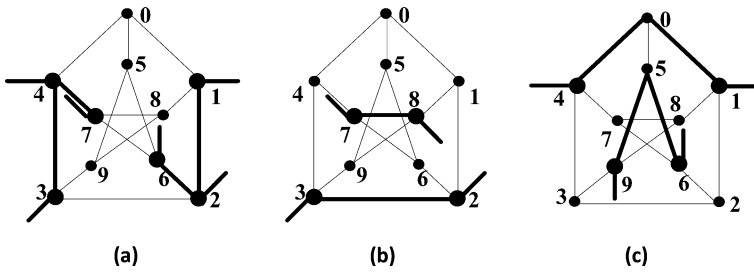


Fig. 12 Distance among nodes adjacent to the external edge

**Appendix**

In the following explanation, an interior angle is the lesser one of the two angles formed at the point where the external edges of two nodes are extended and meet, as shown in part (b) of Fig. 2. For example, the nodes combined with the edge of node 4 and that forming an interior angle of  $45^\circ$  are 3 and 7. The angle mentioned in the following is of course an interior angle.

**Lemma 3** *The distance between nodes combined with external edges other than dimensional edges in the Petersen graph of the basic module is as shown below:*

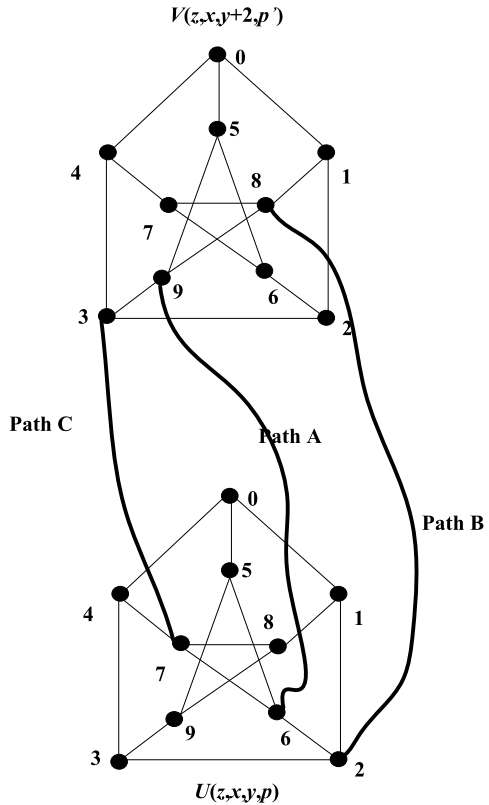
- (1) *If there is node  $p$  combined with an external edge, as well as nodes  $p'$  and  $p''$  combined with two external edges forming an interior angle of  $45^\circ$  with the external edge, the distance between  $p$  and  $p'$  and that between  $p$  and  $p''$  is 1.*
- (2) *The distance between nodes 2 and 3 combined with diagonal edges is 1, and that between nodes 7 and 8 combined with reverse diagonal edges is 1.*
- (3) *The distance between nodes combined with all external edges except (1) and (2) is 2.*

*Proof* In Fig. 12, several examples of Lemma 3 are shown. Part (a) shows (1) of Lemma 3, part (b)–(2), and part (c)–(3). In part (a), the edge combined with node 2 forms an angle of  $45^\circ$  with the edges combined with node 1 and node 6, respectively, and node 2 and node 1, as well as node 2 and node 6, are adjacent to each other; therefore, they are within distance 1. In the same manner, node 4 is adjacent to nodes 7 and 3. Parts (b) and (c) are clear, as shown in the figure, so their explanation is omitted. The demonstration is replaced with Fig. 2, showing an edge design of 3D  $PT(l, m, n)$ , and Fig. 12, showing an example of Lemma 3.  $\square$

**Lemma 4** *From  $U(z, x, y, p)$  to  $V(z', x', y', p')$ , there are two paths  $A$  and  $B$  where  $SA$  and  $SB$  or  $DA$  and  $DB$  are not specified, and if  $lMA = lMB$ , the following properties are shown. (Here, it is assumed that  $z = z'$ , the start node of  $MA$  is  $(z, x, y, 2)$  and the destination node is  $(z, x, y, 8)$ , the start node of  $MB$  is  $(z, x, y, 7)$  and the destination node is  $(z, x, y, 3)$ .)*

- (1) *If  $p = 2, lA \leq lB$ .*

**Fig. 13** Routing path for  $dx = 0, dy \geq 4$



- (2) If  $p \in \{1, 3\}$  and  $p' \neq 3, lA \leq lB$  and if  $p \in \{1, 3\}$  and  $p' = 3, lA > lB$ .
- (3) If  $p \in \{0, 5, 6, 9\}$  and  $p' \in \{2, 3, 4\}, lA > lB$  and if  $p \in \{0, 5, 6, 9\}$  and  $p' \neq \{2, 3, 4\}, lA \leq lB$ .
- (4) If  $p \in \{4, 8\}$  and  $p' \neq 8, lA \geq lB$  and if  $p \in \{4, 8\}$  and  $p' = 8, lA \leq lB$ .
- (5) If  $p = 7, lA \geq lB$ .

*Proof* In Fig. 13,  $MA$  of the path A and  $MB$  of the path B are indicated in thick solid lines and it is assumed that  $lMA = lMB$ . Therefore, if  $lSA + lDA > lSB + lDB, lA > lB$  and if  $lSA + lDA < lSB + lDB, lA < lB$ .

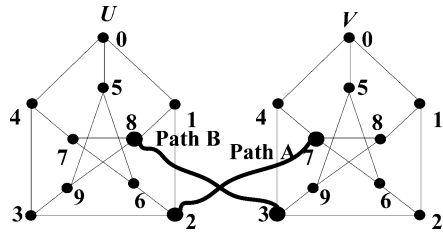
(1) If node  $p = 2, lSA = 0$  and  $lSB = 2$ . Diameter is 2 in the Petersen graph, so  $lDA \leq lDB + 2$ . Therefore,  $lSA + lDA \leq lSB + lDB, lA \leq lB$ .

(2) If node  $p \in \{1, 3\}, lSA = 1$  and  $lSB = 2$ . If  $p' = 3, lDA = 2$  and  $lDB = 0$ . Therefore,  $lSA + lDA > lSB + lDB, lA > lB$ . If  $p' \neq 3, lDA \leq lDB + 1$ . Thus,  $lSA + lDA \leq lSB + lDB, lA \leq lB$ .

(3) If node  $p \in \{0, 5, 6, 9\}, lSA = lSB = 1$ . If  $p' \in \{2, 3, 4\}, lDB < lDA$ . Therefore,  $lB < lA$ . If  $p' \neq \{2, 3, 4\}, lDA \leq lDB$ . Thus,  $lA \leq lB$ .

(4) If node  $p \in \{4, 8\}, lSA = 2$  and  $lSB = 1$ . If  $p' = 8, lDA = 0$  and  $lDB = 2$ . Therefore,  $lSA + lDA < lSB + lDB = lA < lB$ . If  $p' \neq 8, lDB \leq lDA + 1$ . Thus,  $lSA + lDA \geq lSB + lDB, lA \geq lB$ .

**Fig. 14** Routing path for  $dx \geq 4, dy = 0$



(5) If node  $p = 7, l_{SA} = 2$  and  $l_{SB} = 0$ . Diameter is 2 in the Petersen graph, so  $l_{DB} \leq l_{DA} + 2$ . Therefore,  $l_{SA} + l_{DA} \geq l_{SB} + l_{DB}, l_A \geq l_B$ .  $\square$

**Lemma 5** From  $U(z, x, y, p)$  to  $V(z', x', y', p')$ , there are two paths A and B where SA and SB or DA and DB are not specified, and if  $l_{MA} = l_{MB}$ , the following properties are shown. (Here, it is assumed that  $z = z'$ , the start node of MA is  $(z, x, y, 2)$  and the destination node is  $(z, x, y, 7)$ ; it is also assumed that the start node of MB is  $(z, x, y, 8)$  and the destination node is  $(z, x, y, 3)$ .)

- (1) If  $p = 2, l_A \leq l_B$ .
- (2) If  $p \in \{3, 6\}$  and  $p' \neq 3, l_A \leq l_B$  and if  $p \in \{3, 6\}$  and  $p' = 3, l_A > l_B$ .
- (3) If  $p \in \{0, 1, 4, 5\}$  and  $p' \in \{6, 7, 8\}, l_A > l_B$  and if  $p \in \{0, 1, 4, 5\}$  and  $p' \neq \{6, 7, 8\}, l_A \leq l_B$ .
- (4) If  $p \in \{7, 9\}$  and  $p' \neq 7, l_A \geq l_B$  and if  $p \in \{7, 9\}$  and  $p' = 7, l_A < l_B$ .
- (5) If  $p = 8, l_A \geq l_B$ .

*Proof* In Fig. 14, MA of the path A and MB of the path B are indicated in thick solid lines and it is assumed that  $l_{MA} = l_{MB}$ . Therefore, if  $l_{SA} + l_{DA} > l_{SB} + l_{DB}, l_A > l_B$  and if  $l_{SA} + l_{DA} < l_{SB} + l_{DB}, l_A < l_B$ .

(1) If node  $p = 2, l_{SA} = 0$  and  $l_{SB} = 2$ . Diameter is 2 in the Petersen graph, so  $l_{DA} \leq l_{DB} + 2$ . Therefore,  $l_{SA} + l_{DA} \leq l_{SB} + l_{DB}$  and  $l_A \leq l_B$ .

(2) If node  $p \in \{3, 6\}, l_{SA} = 1$  and  $l_{SB} = 2$ . If  $p' = 3, l_{DA} = 2$  and  $l_{DB} = 0$ . Therefore,  $l_{SA} + l_{DA} > l_{SB} + l_{DB} = l_A > l_B$ . If  $p' \neq 3, l_{DA} \leq l_{DB} + 1$ . Thus,  $l_{SA} + l_{DA} \leq l_{SB} + l_{DB}$  and  $l_A \leq l_B$ .

(3) If node  $p \in \{0, 1, 4, 5\}, l_{SA} = l_{SB} = 1$ . If  $p' \in \{6, 7, 8\}, l_{DB} < l_{DA}$ . Therefore,  $l_B < l_A$ . If  $p' \neq \{6, 7, 8\}, l_{DA} \leq l_{DB}$ . Thus,  $l_A \leq l_B$ .

(4) If node  $p \in \{7, 9\}, l_{SA} = 2$  and  $l_{SB} = 1$ . If  $p' = 7, l_{DA} = 0$  and  $l_{DB} = 2$ . Therefore,  $l_{SA} + l_{DA} < l_{SB} + l_{DB} = l_A < l_B$ . If  $p' \neq 7, l_{DB} \leq l_{DA} + 1$ . Thus,  $l_{SA} + l_{DA} \geq l_{SB} + l_{DB}$  and  $l_A \geq l_B$ .

(5) If node  $p = 8, l_{SA} = 2$  and  $l_{SB} = 0$ . Diameter is 2 in the Petersen graph, so  $l_{DB} \leq l_{DA} + 2$ . Therefore,  $l_{SA} + l_{DA} \geq l_{SB} + l_{DB}$  and  $l_A \geq l_B$ .  $\square$

**References**

1. Ergu D, Kou G, Peng Y, Shi Y, Shi Y (2011) The analytic hierarchy process: Task scheduling and resource allocation in cloud computing environment. J Supercomput. doi:10.1007/s11227-011-0625-1

2. Parhami B, Kwai D-M (2001) A unified formulation of honeycomb and diamond networks. *IEEE Trans Parallel Distrib Syst* 12(1):74–80
3. Ni LM, McKinley PK (1993) A survey of wormhole routing techniques in direct networks. *IEEE Comput* 26(2):62–76
4. Parhami B, Rakov M (2005) Perfect difference networks and related interconnection structures for parallel and distributed systems. *IEEE Trans Parallel Distrib Syst* 16(8):714–724
5. Parhami B, Yeh C-H (2000) Why network diameter is still important. In: *Proc int'l conf comm in computing*, pp 271–274
6. Saad Y, Schultz MH (1988) Topological properties of hypercubes. *IEEE Trans Comput* 37(7):867–872
7. Mendia VE, Sarkar D (1992) Optimal broadcasting on the star graph. *IEEE Trans Parallel Distrib Syst* 3(4):389–396
8. Tang KW, Padubidri SA (1994) Diagonal and toroidal mesh networks. *IEEE Trans Comput* 43(7):815–826
9. Latifi S, Srimani PK (1998) A fixed degree regular networks for massively parallel systems. *J Supercomput* 12(3):277–291
10. Zhou S, Du N, Chen B (2006) A new family of interconnection networks of odd fixed degrees. *J Parallel Distrib Comput* 66(5):698–704
11. Moraveji R, Sarbazi-Azad H, Zomaya AY (2011) Performance modeling of Cartesian product networks. *J Parallel Distrib Comput* 71(1):105–113
12. Ghose K, Desai KR (1995) Hierarchical cubic network. *IEEE Trans Parallel Distrib Syst* 6(4), 427–435
13. El-Amawy A, Latifi S (1991) Properties and performances of folded hypercubes. *IEEE Trans Parallel Distrib Syst* 2(1):31–42
14. Efe K (1991) A variation on the hypercube with lower diameter. *IEEE Trans Comput* 40(11):1312–1316
15. Park J-H (1992) Circulant graphs and their application to communication networks. PhD Thesis, Dept of Computer Science, KAIST, Taejon, Korea
16. Yeh C-H, Varvarigos E (1996) Macro-star networks: Efficient low-degree alternatives to star graphs for large-scale parallel architectures. In: *Frontier'96, symp on the frontiers of massively parallel computation*
17. Latifi S, Srimani PK (1996) Transposition networks as a class of fault-tolerant robust networks. *IEEE Trans Comput* 45(2):230–238
18. Lee HO, Kim JS, Park KW, Seo JH (2005) Matrix star graphs: A new interconnection network based on matrix operations. In: *ACSAC 2005. LNCS*, vol 3740, pp 478–487
19. Stojmenovic I (1997) Honeycomb network: Topological properties and communication algorithms. *IEEE Trans Parallel Distrib Syst* 8(10):1036–1042
20. Chen MS, Shin KG (1990) Addressing, routing, and broadcasting in hexagonal mesh multiprocessors. *IEEE Trans Comput* 39(1):10–18
21. Decayeux C, Seme D (2005) 3D hexagonal network: Modeling, topological properties, addressing scheme, and optimal routing algorithm. *IEEE Trans Parallel Distrib Syst* 16(9):875–884
22. Scott SL, Thorson G (1996) The Cray T3E network: Adaptive routing in a high performance 3D toms. In: *HOT interconnects IV*, Stanford University
23. Carle J, Myoupo JF, Stojmenovic I (2001) Higher dimensional honeycomb networks. *J Interconnect Netw* 2(4):391–420
24. Nguyen J, Pezaris J, Pratt GA, Ward S (1994) Three-dimensional network topologies. In: *Proceedings of the first international workshop on parallel computer routing and communication*, pp 101–115
25. Cray Inc (2008) Cray XT3 datasheet. [http://www.cray.com/downloads/Cray\\_XT3\\_Datasheet.pdf](http://www.cray.com/downloads/Cray_XT3_Datasheet.pdf)
26. Cray Inc (2008) Cray XT4 datasheet. [http://www.cray.com/downloads/Cray\\_XT4\\_Datasheet.pdf](http://www.cray.com/downloads/Cray_XT4_Datasheet.pdf)
27. Choo H, Yoo S-M, Youn HY (2000) Processor scheduling and allocation for 3d torus multicomputer systems. *IEEE Trans Parallel Distrib Syst* 11(5):475–484
28. Seo JH, Lee HO, Jang MS (2008) Petersen-torus networks for multicomputer systems. In: *Proc int'l conf of NCM2008*, vol 1, pp 567–571
29. Seo JH, Lee HO (2009) One-to-one embedding between hyper Petersen and Petersen-torus networks. *Int J Grid Distrib Comput* 2(4):27–33
30. Seo JH, Lee HO, Jang MS (2008) Node mapping algorithm between torus and Petersen-torus networks. In: *Proc int'l conf of NCM2008*, vol 2, pp 540–544

31. Seo J-H, Lee H-O (2009) One-to-all broadcasting in Petersen-torus networks for SLA and MLA models. *ETRI J* 31(3):327–329
32. Chartrand G, Wilson RJ (1985) The Petersen graph. In: Harary F, Maybee JS (eds) *Graphs and applications*, pp 69–100
33. Camara JM, Moreto M, Vallejo E, Beivide R, Miguel-Alonso J, Martínez C, Navaridas J (2010) Twisted torus topologies for enhanced interconnection networks. *IEEE Trans Parallel Distrib Syst* 21(12):1765–1778